

A non-invasive method for *in situ* quantification of subpopulation behaviour in mixed cell culture

Ben D MacArthur, Rahul S Tare, Colin P Please, Philip Prescott and Richard O.C Oreffo

J. R. Soc. Interface 2006 **3**, 63-69

doi: 10.1098/rsif.2005.0080

References

[This article cites 23 articles, 6 of which can be accessed free](#)

<http://rsif.royalsocietypublishing.org/content/3/6/63.full.html#ref-list-1>

Email alerting service

Receive free email alerts when new articles cite this article - sign up in the box at the top right-hand corner of the article or click [here](#)

To subscribe to *J. R. Soc. Interface* go to: <http://rsif.royalsocietypublishing.org/subscriptions>

A non-invasive method for *in situ* quantification of subpopulation behaviour in mixed cell culture

Ben D. MacArthur^{1,†}, Rahul S. Tare¹, Colin P. Please², Philip Prescott²
and Richard O. C. Oreffo¹

¹Bone and Joint Research Group, Developmental Origins of Health and Disease, University of Southampton, Southampton General Hospital, Southampton SO16 6YD, UK

²School of Mathematics, University of Southampton, Southampton SO17 1BJ, UK

Ongoing advances in quantitative molecular- and cellular-biology highlight the need for correspondingly quantitative methods in tissue-biology, in which the presence and activity of specific cell-subpopulations can be assessed *in situ*. However, many experimental techniques disturb the natural tissue balance, making it difficult to draw realistic conclusions concerning *in situ* cell behaviour. In this study, we present a widely applicable and minimally invasive method which combines fluorescence cell labelling, retrospective image analysis and mathematical data processing to detect the presence and activity of cell subpopulations, using adhesion patterns in STRO-1 immunoselected human mesenchymal populations and the homogeneous osteoblast-like MG63 continuous cell line as an illustration.

Adhesion is considered on tissue culture plastic and fibronectin surfaces, using cell area as a readily obtainable and individual cell specific measure of spreading. The underlying statistical distributions of cell areas are investigated and mappings between distributions are examined using a combination of graphical and non-parametric statistical methods. We show that activity can be quantified in subpopulations as small as 1% by cell number, and outline behaviour of significant subpopulations in both STRO-1^{+/−} fractions. This method has considerable potential to understand *in situ* cell behaviour and thus has wide applicability, for example in developmental biology and tissue engineering.

Keywords: mathematical analysis; mesenchymal population; adhesion; image cytometry; tissue engineering

1. INTRODUCTION

The last decade has seen an unprecedented insight into the molecular workings of the cell, allowing deconstruction of cellular behaviour with increasing levels of complexity. Additionally, the simultaneous realization of the role of stem-cells in myriad biological processes (McKay 2000; Fuchs & Segre 2000; Weissman 2000; Wagers & Weissman 2004) is redefining the relationship between cellular- and tissue-biology. Such advances re-emphasize the need for a quantitative view of molecular-, cell- and tissue-biology in which conceptual continuity over the full range of spatial length-scales is maintained.

Within homogeneous (pure) cell populations—in which all cells are phenotypically and genetically similar—such analysis can begin to be undertaken *in vitro* since there is a direct relationship between cellular- and population-behaviour, allowing *average* individual cell behaviour to be directly deduced from population parameters. Thus, homogenous continuous

cell lines provide a robust tool for determining simplified relationships between molecular-, cell- and population-level parameters and the scaling that exists between them. However, homogeneous continuous cell-lines provide a rather restricted archetype for the study of heterogeneous primary tissues—which consist of a mix of phenotypically distinct cell types—particularly in situations where indistinct, functionally significant subpopulations are present (for example in stem-cell systems). Quantification of the *in situ* behaviour of such populations is now pivotal to advance understanding in many areas, including developmental biology and regenerative medicine.

In order to address this need, we have examined a generic, minimally invasive method which combines fluorescence cell labelling, retrospective image analysis and mathematical data processing to investigate *in situ* behaviour in heterogeneous primary tissue samples. Central to this methodology is that (i) cells are accurately imaged using appropriate microscopy, (ii) these images are exported in an appropriate format for image analysis, (iii) image analysis is performed on an unbiased, representative portion of the population and (iv) images

[†]Author for correspondence (bdm@soton.ac.uk).

are converted to numerical datasets in an appropriate format for statistical analysis—issues which are central to the field of image cytometry generally (Chieco *et al.* 2001). This current work focuses primarily on statistical analysis of the derived numerical datasets.

Crucially, this method does not analyse individual images for patterns, but rather detects patterns of subpopulation *behaviour* by statistical comparison across datasets. Automated pattern identification software are described elsewhere (for example Hu & Murphy 2004).

The central concept is as follows: the statistical distributions of cell-level parameters (e.g. cell area) in a population are determined by the particular collection of cell-types in that population and may be described mathematically by variables such as average (for example, the mean), spread (for example, the standard deviation) and shape (for example, skew). If the population is heterogeneous, consisting of a number of distinct cell-types, changes in the environment may affect each cell-type in the population in distinctly different ways, resulting in a qualitative change in the shape—not simply the average and spread—of the underlying distribution. Thus, distributional shape changes under environmental perturbation relate to the activity of cell subpopulations. Conversely, a homogeneous response—in which all cells in the population respond in a similar manner—is characterized by invariance of distributional shape under environmental perturbation.

Similarly, comparison of the distributions of cellular parameters arising from different tissues (or tissue fractions) allows clarification of the compositional disparity between populations. In particular, comparison of the distributions of cellular parameters from a known homogeneous population—in this case we use the continuous cell-line MG63—with those of an unknown population allows quantification of the level of compositional purity of the unknown tissue.

Determination of the percentile points of a dataset provides a simple way to elucidate distributional structure (the k th percentile is that point, below which k per cent of the data lies; Rahman 1968; DeGroot 1989). Consequently, percentile–percentile (P–P) plots constitute a sensitive non-parametric means to compare relationships between underlying statistical distributions in different sets of data (Chambers *et al.* 1983; Hoaglin *et al.* 1983). Crucially, the P–P plot of two samples from populations which follow the same distribution will be linear even though the underlying distributions may have different averages and spreads. Conversely, if the distributions are significantly different in shape, then the P–P plot will be nonlinear with the degree of nonlinearity directly relating to the nature of the distributional disparity between the two datasets.

Thus, in this study, P–P plots were used to examine the relationships between adhesion profiles of distinct mesenchymal populations from human bone marrow on tissue culture plastic and fibronectin. Additionally, quantile–quantile (Q–Q) plots were also used to compare distributions; however, P–P plots are presented since they utilize the full range of the data, while Q–Q plots emphasize tails.

Mesenchymal populations were chosen since they are a relatively available and clinically effective (Wakitani *et al.* 2002) heterogeneous bone marrow-derived cell source, with the capacity to differentiate along a number of lineages (Pittenger *et al.* 1999; Jiang *et al.* 2002).

In order to isolate further cell populations from marrow, antibodies can be utilized (Simmons & Torok-Storb 1991; Haynesworth *et al.* 1992; Bruder *et al.* 1998; Bianco & Robey 2001). For example, STRO-1 recognizes a trypsin-resistant cell surface antigen present on a subpopulation of bone marrow cells, including a predominant proportion of the osteogenic high growth- and differentiation-potential mesenchymal stem-cell and colony forming units-fibroblastic populations (Simmons & Torok-Storb 1991; Gronthos *et al.* 1994). Consequently, STRO-1 selected and unselected fractions provide disparate mixed-cell populations from the same source and are therefore ideal for comparative studies on tissue formation and heterogeneity.

The aims of the present study were to examine patterns of adhesion in heterogeneous cell populations, and to determine how P–P mappings between underlying distributions elucidate the behaviour of specific tissue subpopulations *in situ*. A particular aim was to use this method to investigate patterns of adhesion in selected mesenchymal ($STRO-1^{+/-}$) populations on tissue culture plastic and fibronectin, as both an example to illustrate the proposed method and as a means to begin to understand *in situ* regulation of tissue function for bone tissue engineering applications.

2. MATERIAL AND METHODS

Tissue culture reagents (DMEM, α MEM, Fetal Calf Serum), and all other biochemical reagents were obtained from Sigma-Aldrich, UK, unless otherwise stated. Cell Tracker Green CMFDA (5-chloromethyl-fluorescein diacetate) was purchased from Molecular Probes, Leiden, The Netherlands.

2.1. Magnetic activated cell sorting

A bone marrow sample (72-year-old male) was obtained from a haematologically normal patient undergoing routine total hip replacement surgery (in order to demonstrate the efficacy of this method, it was only necessary to consider tissue fractions from one patient. Significance is derived from the use of multiple tissue fractions and the large number of cells considered per fraction). Only tissue that would have been discarded was used, with the approval of the Southampton & South West Hants Local Research Ethics Committee. $STRO-1^+$ cells were isolated as described by Stewart *et al.* (1999). All studies were conducted using passage 1 mesenchymal populations.

2.2. Cell culture on fibronectin and tissue culture plastic

All cells ($STRO-1^{+/-}$ and MG63 [ECACC, Salisbury, UK]) (2×10^7) were incubated with CMFDA for 2 h. CMFDA is only incorporated into the cell cytoplasm of

viable cells and remains present through at least four cell divisions (Johnson 1998). The media were then replaced and the cells incubated for an additional hour. Following trypsinization, cells were centrifuged and re-suspended in serum-free media. Cells (4000) were added to each well of standard tissue culture plastic (TCP) and fibronectin (FN) coated 24-well plates (Bibby Sterilin, UK [TCP], Becton Dickinson, UK [FN]) so that six wells were occupied by each cell type. Cells were then incubated 37 °C and 5% CO₂ with those seeded on TCP being maintained in media containing 10% fetal calf serum and those on FN being maintained in serum-free media. After 24 h, media were removed and cells were fixed for 15 min in cold 95% ethanol and left to air dry. Fluorescence images of the fixed cells were then taken.

2.3. Fluorescence microscopy and image analysis

Images were taken using a Leica TCS SP2 confocal laser scanning microscope incorporating an inverted Leica DM IRBE inverted microscope equipped with a fluorescence filter enabling fluorescent imaging (using 488 nm wavelength blue light) using integral Leica confocal software. Three to five random images were taken per well at 10 magnification (image size 2.56 × 10⁶ µm²), resulting in 18–30 images per cell type per surface.

Cell area measurements were then obtained with the assistance of computerized image analysis using the KS400 software package (Image Associates, Bicester, UK). Briefly, using TIFF images from confocal microscopy, binary images of cells were created employing user-interactive thresholding based upon red–green–blue colour balance. The green channel was used since cells were labelled with CMFDA. The system was calibrated using a slide micrometer and cell areas were obtained from analysis of the binary images using algorithms integral to the KS400 software. In order to only assess the effect of cell–substratum adhesion on cell area, special care was taken to ensure that cells which were touching were excluded in analysis, as were those cells which were not obviously in the plane of focus and those cells near to, or touching, the edge of the well. Areas of upwards of 300 to greater than 600 cells were randomly obtained per sample per surface to ensure statistical significance ($n_{\text{STRO-1+}/\text{TCP}}=337$; $n_{\text{STRO-1+}/\text{FN}}=519$; $n_{\text{STRO-1-}/\text{TCP}}=519$; $n_{\text{STRO-1-}/\text{FN}}=582$; $n_{\text{MG63}/\text{TCP}}=690$; $n_{\text{MG63}/\text{FN}}=526$).

2.4. Statistical analysis

Percentiles (1–99 inclusive) were found for each dataset. The 100th percentile was excluded from analysis since it, unlike all the other percentile points, relies solely on one observation—that of the largest cell. Percentiles for various datasets were then plotted against each other to obtain percentile–percentile (P–P) plots which illustrate the nature of the relationship between the two sets of data. Plots of variations in response to FN with percentile were then used to investigate the nature of any nonlinearity and to quantify the response of specific subpopulations.

Least-squares regression was used to determine the best linear fit for each appropriate data subset and combination of P–P data.

The distribution of cell areas was further investigated using the Anderson–Darling test, an outlier sensitive non-parametric test which allows comparison of data with expected values from a variety of known distributions (Sprent & Smeeton 2005). All statistical analysis was undertaken using the statistical software packages Minitab, SigmaPlot and SPSS.

3. RESULTS

Cell attachment and spreading were initially assessed by photomicroscopy. On both surfaces minimal cell detachment and death were observed, with the majority of cells displaying a spread and adherent morphology (figure 1). Cell viability was confirmed by intense green fluorescence of the cells as a consequence of uptake of the CMFDA fluorescent probe.

Although ethanol fixation may cause cellular dehydration and subsequent cell volume shrinkage, it is not expected to have a significant effect on cell–substratum area, since the adherent morphology of all cells demonstrates that adhesive attachments are maintained following fixation (figure 1). Furthermore, if there is any cell–substratum area shrinkage due to fixation then it is uniform across all cells in a particular population. This is demonstrated by the linearity of the P–P plot of MG63 response to FN (figure 3). Since all cells were fixed using the same protocol, fixation is not expected to contribute significantly to the degree of nonlinearity of any of the P–P plots.

Comparison of all datasets with the normal distribution, using the Anderson–Darling test, showed that cell areas do not follow a normal distribution in any of the populations examined ($p < 0.005$ in all cases), confirming the need for non-parametric statistical analysis.

3.1. Heterogeneity of composition

Comparison of the distributions of cell areas in the STRO-1^{+/−} populations with that of the archetypical homogeneous cell line, MG63, elucidates the degree of compositional purity of the STRO-1^{+/−} fractions. P–P plots of the STRO-1^{+/−} fractions against MG63 on both surfaces (figure 2) are nonlinear showing that neither fraction is pure, with both containing a mixture of distinct cell types.

Comparison of the distribution of cell areas in the STRO-1^{+/−} populations with each other elucidates the degree of compositional disparity between them. On both surfaces, P–P plots of the STRO-1⁺ against the STRO-1[−] fractions are also nonlinear showing that, in addition to being heterogeneous in composition, these two populations are also compositionally distinct from each other, containing a measurably different collection of cell types (figure 2).

3.2. Heterogeneity of response

Comparison of the distributions of cell areas in a particular population under different environmental

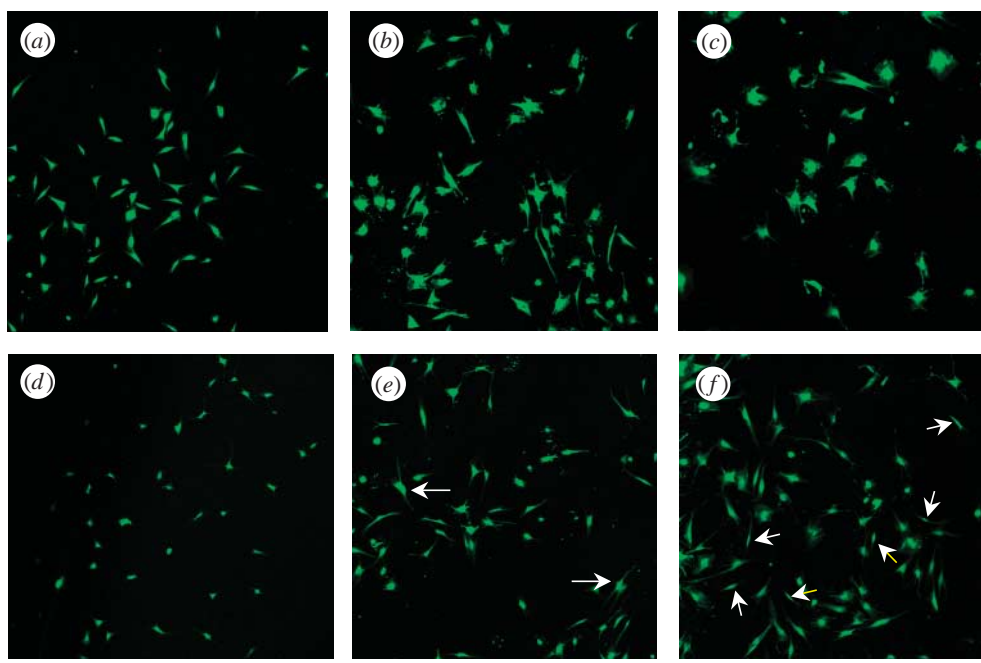


Figure 1. Cell adhesion on tissue culture plastic (row 1, *a*–*c*) and fibronectin (row 2, *d*–*f*). MG63 adhesion is in column 1 (*a*, *d*). STRO-1[−] adhesion is in column 2 (*b*, *e*): arrows highlight cells in the 90th percentile (P_{90}). STRO-1⁺ adhesion is in column 3 (*c*, *f*): white arrows highlight cells in the first quartile (Q_1), yellow arrows highlight cells in the lower five percentile (P_5).

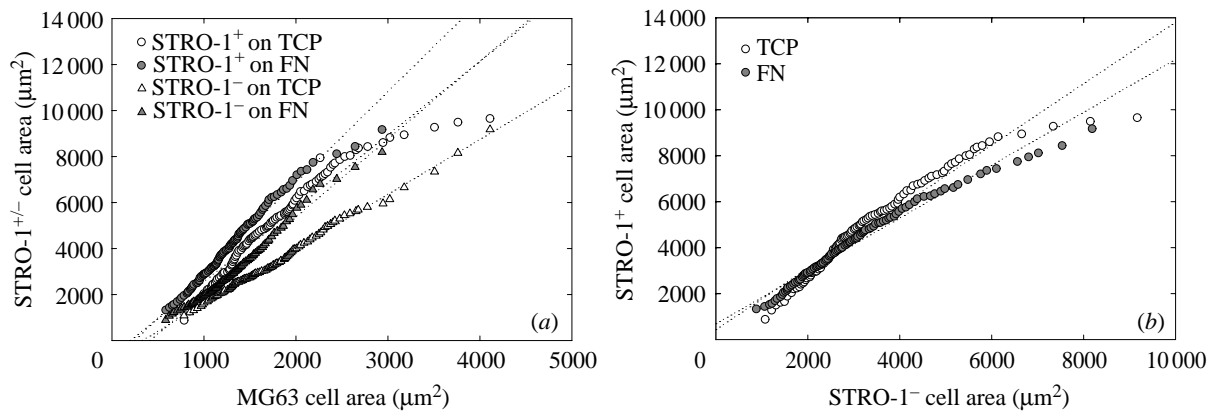


Figure 2. (a) P–P plots of STRO-1^{+/−} composition are nonlinear, showing distinct differences between MG63 and STRO-1^{+/−} populations and suggesting that STRO-1^{+/−} populations are not pure. (b) P–P plots of STRO-1^{+/−} disparity are nonlinear, suggesting that these populations are disparate in distribution of cell types. The same qualitative trends are found on both surfaces. Dotted lines show linear least-square regressions for the full datasets.

conditions elucidates heterogeneity of response (the degree to which different subpopulations behave in a measurably different manner to each other within the population).

The response of the MG63 cell line to surface modification with FN was homogenous (figure 3), as evidenced by the linear relationship in the P–P plot. Thus, the MG63 population response to FN is directly proportional to the individual cellular response to FN, and translation between population- and cellular-biology reduces to determination of appropriate scale factors. This is a definitive feature of the continuous cell line. The absence of any subpopulation activity in the MG63 population provides a negative control population, by which subpopulation activity in the STRO-1^{+/−} fractions may be assessed.

Conversely, P–P plots of the response of the STRO-1^{+/−} populations to FN are nonlinear. Since the P–P plot of MG63 response to FN is linear we conclude that this nonlinearity is due to subpopulation behaviour rather than a nonlinear response from a homogeneous population. In both cases, the nonlinearity is localized to distinct percentile regions, suggesting that the STRO-1^{+/−} populations contain distinct subpopulations which exhibit differential responses to surface modification with FN.

In order to further investigate the nature of this heterogeneity we plotted variations in response to FN with percentile, as determined by the percentage difference between the k th percentile on FN, P_k^{FN} , and the k th percentile on TCP, P_k^{TCP} , by comparison with percentiles on TCP. That is, we consider how the

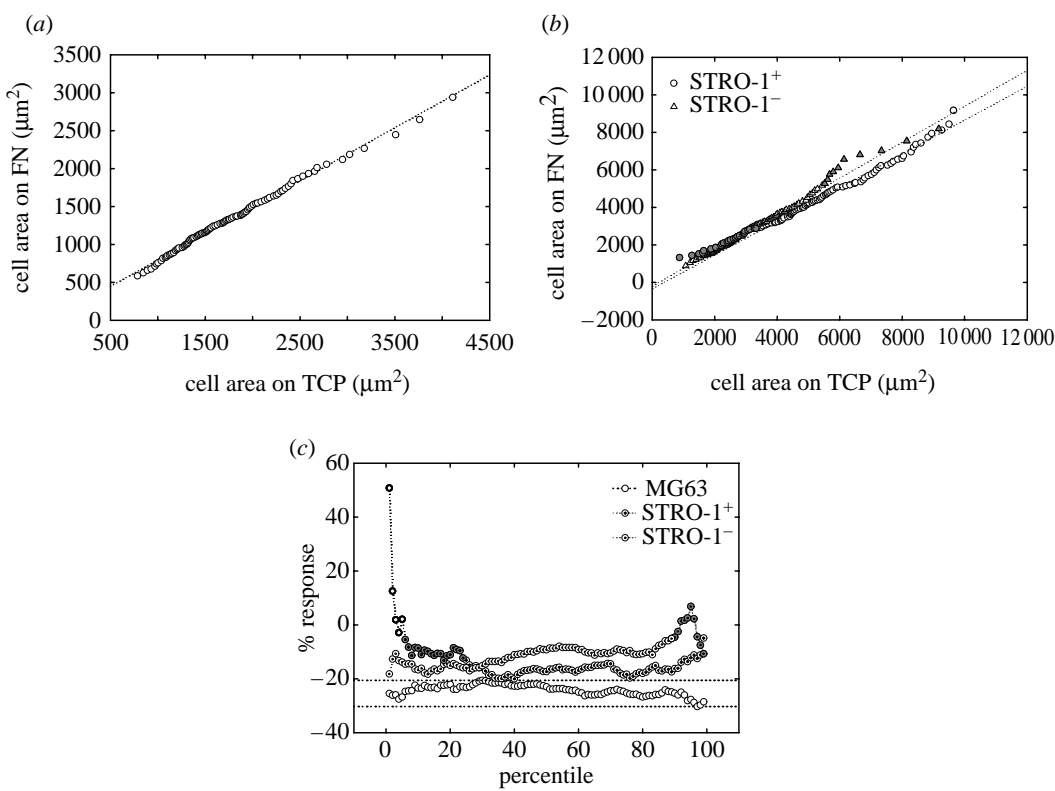


Figure 3. (a) P-P plot of MG63 response to FN shows a strong linear relationship throughout, suggesting a homogenous response by the MG63 population to environmental modification with FN. (b) P-P plots of STRO-1^{+/−} responses to FN are nonlinear, suggesting subpopulation variations in response. Dotted lines show linear least-square regressions (from P_{26} to P_{99} for STRO-1⁺ and from P_1 to P_{89} for STRO-1[−]). (c) STRO-1^{+/−} response to FN by percentile: the response of STRO-1⁺ cells in the lower quartile (grey) is measurably different to the rest of the STRO-1⁺ population. Furthermore, the response of STRO-1⁺ cells in the smallest 5% (black) is measurably different to the rest of the lower quartile subpopulation. Behaviour of STRO-1[−] cells in the 90th percentile (grey) is measurably different to the rest of the STRO-1[−] population. The small variation of MG63 response over the full percentile range (between the dotted lines) quantifies inherent homogeneous variability and experimental error. In this figure, a negative response corresponds to cell shrinkage, while a positive response corresponds to cell spreading.

quantity $100 \times [(P_k^{\text{FN}} - P_k^{\text{TCP}}) / (P_k^{\text{TCP}})]$ varies with percentile.

Variations in response to FN with percentile in the MG63 population were small (a 9.7% range in response was observed) and are representative of inherent homogeneous population variability and experimental error. Conversely, the range of response in both the STRO-1^{+/−} fractions was considerably larger (a 25.2% range in response was observed in the STRO-1[−] fraction, while a 70.8% range in response was observed in the STRO-1⁺ fraction). Thus, by centring this 9.7% bound about the median response in each of the STRO-1^{+/−} populations, those areas in which there is significant behaviour—that is, behaviour which is not attributable to intrinsic experimental or pure population variability—can be determined. Clear trends of variations in the STRO-1^{+/−} population responses to FN in excess of this range represent significant behaviour of cell subpopulations.

In the case of the STRO-1[−] fraction, the large variation in response in the 90th percentile (P_{90}) shows that these cells responded in a measurably different way to FN than the rest of the population (figure 3). Mean response in P_{90} was a 1.5% decrease in cell area, whereas the mean response over the rest of the population was an 11.9% decrease in cell area, relative

to areas on TCP. Linear least-squares regression from P_1 to P_{89} shows a good fit to the data, suggesting that the remainder of the STRO-1[−] fraction respond to FN in a uniform manner.

In the case of the STRO-1⁺ fraction, the large variation in response in the lower quartile (Q_1 , the smallest 25%) shows that these cells responded in a measurably different way to FN than the rest of the population (figure 3). The Q_1 -subpopulation can be decomposed further by imposing the bounds of reasonable variation on this subpopulation and again looking for trends in response in excess of this range. Doing so shows that the smallest 5% of cells (P_5) respond in a measurably different way to FN than the rest of the Q_1 -subpopulation.

The mean P_5 -STRO-1⁺ response to FN was a 12.9% increase in cell area. The mean response over the remainder of the Q_1 -subpopulation was a 10.2% decrease in cell area, while the mean response over the remainder of the population as a whole was a 16.4% decrease in area (all by comparison with areas on TCP). Linear least-squares regression for all data points within the bounds of intrinsic experimental variation (all except Q_1) shows a good fit to the data, suggesting that the remainder of the STRO-1⁺ fraction responded to FN in a uniform manner.

4. CONCLUSIONS

In this study, we have presented a sensitive analytical method to quantify *in situ* behaviour of subpopulations in heterogeneous tissues, using patterns of adhesion in human mesenchymal populations as a biologically and clinically relevant example. By comparison with adhesion patterns in the homogeneous osteoblast-like MG63 population, we have demonstrated that both STRO-1⁺⁻ fractions are heterogeneous in their composition, containing a measurably different collection of cell types. We have additionally demonstrated that this method is effective in quantifying the activity of significant subpopulations in both STRO-1⁺⁻ fractions, and also shown that significant subpopulations do not exist in the MG63 cell line. Crucially, this method uses fluorescence cell labelling in combination with image analysis and mathematical data processing to detect the presence and activity of cell subpopulations retrospectively, in a non-invasive manner. Although we have considered cell area as an illustrative example, recent advances in fluorescence cell- and protein-labelling (Miyawaki *et al.* 2003) mean that this method can be used to characterize cell behaviour using a wide variety of biochemical-, protein- or alternative phenotypic-markers within any mixed cell population.

Since the statistical distributions of subpopulations behaviours will almost certainly overlap, a certain degree of subpopulation mixing is inevitable and precise demarcation between subpopulations is not possible. This method therefore assesses subpopulation activity based upon trends in response in excess of intrinsic experimental bounds (not simply on the basis of single percentile points outside of these bounds). For this reason, accurate quantification of the activity of subpopulations which occupy less than a few percentiles cannot reasonably be undertaken. However, in combination with additional selection procedures smaller subpopulations can be identified. In this case, since selection using the STRO-1 antibody from adult marrow isolates approximately 7% of the total adherent cell population (Howard *et al.* 2002), we have assessed behaviour of marrow subpopulations with incidence considerably smaller than 1% by total adherent cell number.

P_5 -STRO-1⁺, Q_1 -STRO-1⁺ and P_{90} -STRO-1⁻ cells are marked on figure 1. Both the Q_1 -STRO-1⁺ and P_{90} -STRO-1⁻ subpopulations appear to form morphologically distinct subpopulations, while the P_5 -STRO-1⁺ fraction appears be morphologically indistinct from the rest of the Q_1 -STRO-1⁺ subpopulation. The exact nature of these subpopulations remains undetermined. For example, due to their relatively small size and incidence the Q_1 -STRO-1⁺ fraction could represent those cells which are immediately post-mitotic; alternatively, they could form a phenotypically distinct subpopulation. Techniques such as gate analysis or use of cell cycle inhibitors to synchronize cells prior to isolation may further elucidate the nature of these subpopulations.

Previously, a role for FN in the regulation of the early stages of osteogenesis has been suggested, with regulation being orchestrated through key Arg-Gly-

Asp (RGD) integrin receptors (Mousri *et al.* 1996; Mousri *et al.* 1997). In particular, the $\alpha_5\beta_1$ fibronectin-specific integrin has been implicated in this process in both primary-cell and MG63 cultures (Dedhar *et al.* 1987; Dedhar 1989a,b; Mousri *et al.* 1997). In addition, studies from Stewart and co-workers and Gronthos *et al.* indicate that it is possible to subtype the STRO-1⁺⁻ populations using dual-colour fluorescence-activated cell sorting (FACS) for alkaline phosphatase (ALP is a marker of osteogenesis) and STRO-1 expression (Gronthos *et al.* 1999; Stewart *et al.* 1999). Consequently, human bone cell populations can be divided into four fractions: STRO-1⁺/ALP⁻, STRO-1⁻/ALP⁻, STRO-1⁺/ALP⁺ and STRO-1⁻/ALP⁺. Cells exclusively expressing the STRO-1 antigen (STRO-1⁺/ALP⁻) were observed to be pre-osteoblastic, while the STRO-1⁻/ALP⁺ and STRO-1⁻/ALP⁻ populations appeared to represent more fully differentiated osteoblasts. The STRO-1⁺/ALP⁺ subset were believed to represent an intermediate stage of osteoblast development. Thus, the STRO-1 antibody is thought to select a mesenchymal stem-cell/progenitor enriched population (Simmons & Torok-Storb 1991; Gronthos *et al.* 1994) with the STRO-1⁻ fraction containing more terminally differentiated cell types. It may therefore be expected that the STRO-1⁻ fraction will express a more uniform pattern of adhesion and response to FN than the STRO-1⁺ fraction. This is indeed confirmed by the greater linearity of the STRO-1⁻ P-P plots in figures 2 and 3.

These results illustrate that in heterogeneous tissues, population-level parameters, such as average cellular response to FN, cannot reasonably be associated with behaviour of any specific cell subpopulation *per se*, since averaging over the population as a whole obscures biological detail. Rather, population parameters are better interpreted as weighted averages across any subpopulations present. Additionally, those molecular factors which are associated with changes in cell behaviour (for example, gene- and protein-expression) are also best related to population averages by weighting over the same cell subpopulations. Quantitative translation between molecular- and cellular-biology and tissue-biology necessarily requires *a priori* knowledge of tissue structure.

The outlined method provides a novel and non-invasive means to determine population structure and thus can be used in combination with other well-established techniques—such as quantitative polymerase chain reaction (QPCR), western blot and histological analysis—to help understand complex biological relationships across multiple length-scales. Due to the widespread need for such tools in cell- and tissue-culture, for example in regenerative medicine and developmental biology, many fruitful applications of this method are envisaged.

REFERENCES

Bianco, P. & Robey, G. P. 2001 Stem cells in tissue engineering. *Nature* **414**, 118–121. (doi:10.1038/35102181)
 Bruder, S. P., Ricalton, N. S., Boynton, R. E., Connolly, T. J., Jaiswal, N., Zaia, J. & Barry, F. P. 1998 Mesenchymal stem

cell surface antigen SB-10 corresponds to activated leukocyte cell adhesion molecule and is involved in osteogenic differentiation. *J. Bone Miner. Res.* **13**, 655–663.

Chambers, J. M., Cleveland, W. S., Kleiner, B. & Tukey, P. A. 1983 Graphical methods for data analysis. Belmont, CA: Wadsworth.

Chieco, P., Jonker, A. & Van Noorden, C. J. F. 2001 *Image cytometry*. Oxford, UK: BIOS Scientific Ltd.

Dedhar, S. 1989a Regulation of expression of the cell adhesion receptors, integrins, by recombinant human interleukin-1 beta in human osteosarcoma cells: inhibition of cell proliferation and stimulation of alkaline phosphatase activity. *J. Cell. Physiol.* **138**, 291–299. (doi:10.1002/jcp.1041380210)

Dedhar, S. 1989b Signal transduction via the beta 1 integrins is a required intermediate in interleukin-1 beta induction of alkaline phosphatase activity in human osteosarcoma cells. *Exp. Cell Res.* **183**, 207–214. (doi:10.1016/0014-4827(89)90430-8)

Dedhar, S., Argraves, W. S., Suzuki, S., Ruoslahti, E. & Pierschbacher, M. D. 1987 Human osteosarcoma cells resistant to detachment by an Arg-Gly-Asp-containing peptide overproduce the fibronectin receptor. *J. Cell Biol.* **105**, 1175–1182. (doi:10.1083/jcb.105.3.1175)

DeGroot, M. H. 1989 Probability and statistics. Cambridge: Addison-Wesley.

Fuchs, E. & Segre, J. A. 2000 Stem cells: a new lease on life. *Cell* **100**, 143–155. (doi:10.1016/S0092-8674(00)81691-8)

Gronthos, S., Graves, S. E., Ohta, S. & Simmons, P. J. 1994 The STRO-1+ fraction of adult human bone marrow contains the osteogenic precursors. *Blood* **84**, 4164–4173.

Gronthos, S., Zannettino, A. C., Graves, S. E., Ohta, S., Hay, S. J. & Simmons, P. J. 1999 Differential cell surface expression of the STRO-1 and alkaline phosphatase antigens on discrete developmental stages in primary cultures of human bone cells. *J. Bone Miner. Res.* **14**, 47–56.

Haynesworth, S. E., Baber, M. A. & Caplan, A. I. 1992 Cell surface antigens on human marrow-derived mesenchymal cells are detected by monoclonal antibodies. *Bone* **13**, 69–80. (doi:10.1016/8756-3282(92)90363-2)

Hoaglin, D. C., Mosteller, F. & Tukey, J. W. 1983 Understanding robust and exploratory data analysis. New York: Wiley.

Howard, D., Partridge, K., Yang, X., Clarke, N. M., Okubo, Y., Bessho, K., Howdle, S. M., Shakesheff, K. M. & Oreffo, R. O. 2002 Immunoselection and adenoviral genetic modulation of human osteoprogenitors: *in vivo* bone formation on PLA scaffold. *Biochem. Biophys. Res. Commun.* **299**, 208–215. (doi:10.1016/S0006-291X(02)02561-5)

Hu, Y. & Murphy, R. F. 2004 Automated interpretation of subcellular patterns from immunofluorescence microscopy. *J. Immunol. Methods* **290**, 93–105. (doi:10.1016/j.jim.2004.04.011)

Jiang, Y. *et al.* 2002 Pluripotency of mesenchymal stem cells derived from adult marrow. *Nature* **418**, 41–49.

Johnson, I. 1998 Fluorescent probes for living cells. *Histochem. J.* **30**, 123–140. (doi:10.1023/A:1003287101868)

McKay, R. 2000 Stem cells—hype and hope. *Nature* **406**, 361–364. (doi:10.1038/35019186)

Miyawaki, A., Sawano, A. & Kogure, T. 2003 Lighting up cells: labelling proteins with fluorophores. *Nat. Cell Biol.* **5** (Suppl. 1), S1–S7.

Moursi, A. M., Damsky, C. H., Lull, J., Zimmerman, D., Doty, S. B., Aota, S. & Globus, R. K. 1996 Fibronectin regulates calvarial osteoblast differentiation. *J. Cell Sci.* **109**, 1369–1380.

Moursi, A. M., Globus, R. K. & Damsky, C. H. 1997 Interactions between integrin receptors and fibronectin are required for calvarial osteoblast differentiation *in vitro*. *J. Cell Sci.* **110**, 2187–2196.

Pittenger, M. F., Mackay, A. M., Beck, S. C., Jaiswal, R. K., Douglas, R., Mosca, J. D., Moorman, M. A., Simonetti, D. W., Craig, S. & Marshak, D. R. 1999 Multilineage potential of adult human mesenchymal stem cells. *Science* **284**, 143–147. (doi:10.1126/science.284.5411.143)

Rahman, N. A. 1968 A course in theoretical statistics. London: Griffin.

Simmons, P. J. & Torok-Storb, B. 1991 Identification of stromal cell precursors in human bone marrow by a novel monoclonal antibody, STRO-1. *Blood* **78**, 55–62.

Sprent, P. & Smeeton, N. C. 2005 Applied nonparametric statistical methods. London: Chapman & Hall.

Stewart, K., Walsh, S., Screen, J., Jefferiss, C. M., Chainey, J., Jordan, G. R. & Beresford, J. N. 1999 Further characterization of cells expressing STRO-1 in cultures of adult human bone marrow stromal cells. *J. Bone Miner. Res.* **14**, 1345–1356.

Wagers, A. J. & Weissman, I. L. 2004 Plasticity of adult stem cells. *Cell* **116**, 639–648. (doi:10.1016/S0092-8674(04)00208-9)

Wakitani, S., Imoto, K., Yamamoto, T., Saito, M., Murata, N. & Yoneda, M. 2002 Human autologous culture expanded bone marrow mesenchymal cell transplantation for repair of cartilage defects in osteoarthritic knees. *Osteoarthritis Cartilage* **10**, 199–206. (doi:10.1053/joca.2001.0504)

Weissman, I. L. 2000 Stem cells: units of development, units of regeneration, and units in evolution. *Cell* **100**, 157–168. (doi:10.1016/S0092-8674(00)81692-X)